ELSEVIER

Spatial synchrony in host–parasitoid models using aggregation of variables

Tri Nguyen-Huu [a,d,*], Christophe Lett [b], Pierre Auger [a,c],
Jean-Christophe Poggiale [d]

[a] *Institut des Systèmes Complexes, Ecole Normale Supérieure de Lyon, 69364 Lyon cedex 07, France*
[b] *Laboratoire de Biométrie et Biologie Evolutive (UMR 5558), CNRS, Université Lyon 1, 43 Bd du 11 novembre,
69622 Villeurbanne Cedex, France*
[c] *UR GEODES, IRD, 32 av. H. Varagnat, 93143 Bondy Cedex, France*
[d] *Centre d'Océanologie de Marseille, Laboratoire d'Océanographie et de Biogéochimie,
Campus de Luminy – Case 901, 13288 Marseille Cedex 09, France*

Abstract

We consider a host–parasitoid system with individuals moving on a square grid of patches. We study the effects of increasing movement frequency of hosts and parasitoids on the spatial dynamics of the system. We show that there exists a threshold value of movement frequency above which spatial synchrony occurs and the dynamics of the system can be described by an aggregated model governing the total population densities on the grid. Numerical simulations show that this threshold value is usually small. This allows using the aggregated model to make valid predictions about global host–parasitoid spatial dynamics.
© 2006 Elsevier Inc. All rights reserved.

Keywords: Host–parasitoid models; Aggregation of variables; Two-dimensional network; Movement frequency; Spatial synchrony

* Corresponding author. Address: Institut des Systèmes Complexes, Ecole Normale Supérieure de Lyon, 69364 Lyon cedex 07, France. Tel.: +33 4 72 43 13 44; fax: +33 4 72 43 13 88.
 E-mail address: tri.nguyen-huu@ens-lyon.fr (T. Nguyen-Huu).

1. Introduction

Many field observations have shown that the dynamics of different sub-populations of the same population located at different places were synchronised. This spatial synchrony has been observed for different species of insects [1,2], fishes [3], birds [4,5], mammals [6,7], turtles [8], trees [9] and viruses [10]. Although it decreases with the distance between populations, this synchrony effect can be observed for important distances, from kilometres to thousands of kilometres [11–13].

Two main causes have been investigated to explain this spatial synchrony effect. The first one is known as the Moran effect resulting from environmental correlations [14]. The second cause is dispersal [15]. The two processes can contribute to spatial synchrony at the same time [16]. The aim of this work is to use models to investigate the effect of local dispersal on spatial synchrony of a host–parasitoid system.

Building detailed models implies considering an important number of variables, which makes a mathematical analysis difficult. Models incorporating slow and fast processes allow some simplifications [17–19]. Aggregation of variables methods are aimed at reducing the dimension of a mathematical model to make it available for analytical study. Aggregation of variables of a system consists in the consideration of a small number of global variables and the system describing their dynamics. When the dynamics of the global variables is exactly the same in the aggregated model as in the initial model (referred to as the complete model), it is called perfect aggregation [20]. When perfect aggregation is not possible, approximate aggregation methods are used [21–23]. The consistency of the global variables in the complete and the aggregated systems is then only approximate. Those methods can take advantage of multiple time scales in a system, for continuous time [24–26] as well as for discrete time models [27,28]. The aggregated model is obtained from the complete model by making the approximation that the fast system tends to some stable attractor, for example an equilibrium point. This approximation is valid when the aggregated model is structurally stable and the difference between the two time scales is large. In the case of spatial population dynamics with fast symmetric dispersal and slow local interactions, the aggregated model is obtained by making the approximation that local sub-populations become synchronous. Therefore, the aggregated model is a good tool to explore spatial synchrony.

Spatial host–parasitoid dynamics models usually combine two sub-models, one describing local host–parasitoid interactions on each patch and the other describing dispersal among patches (see [29]). Those models were mostly developed to study the dynamics, the persistence [30] and stability [31,32] of the host–parasitoid population. Reeve [33] showed that for the non-persistent Nicholson–Bailey models with individuals moving to any other patch, persistence could only occur with density-dependant parasitism. Hassell et al. [30] and Comins et al. [34] considered spatial environment as a two-dimensional network of patches connected by dispersal on the eight nearest neighbours. For a sufficiently large grid, the system could persist without any other stabilizing mechanism [34] but the localised nature of dispersal [35] which allows asynchrony between populations [36] and the emergence of spatial structures such as spiral waves, chaotic dynamics or crystal structures [30].

These models involved a single time scale in the sense that between two generations, local interactions as well as dispersal processes were performed one time. Some models consider one global
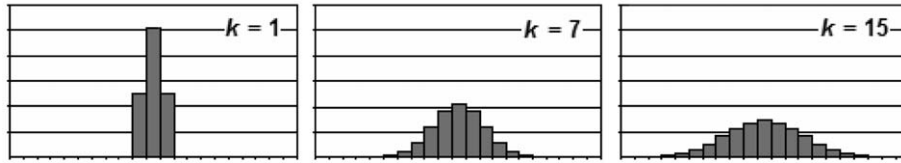
Fig. 1. Densities of individuals after k events of dispersal for $k = 1$, 7 and 15. All individuals start on the centre patch, and 50% of them move to an adjacent patch at each event of dispersal.

event of dispersion [37]. But most models use the hypothesis of a single event of random dispersal on the eight neighbouring patches [38]. However, in some situations, insects can reach further patches. This is likely to occur for most host–parasitoid associations involving winged adults like wasps, butterflies, flies or midges [39,40]. In a recent work, Huang and Diekmann [41] considered a dispersal process consisting of two events: after landing on a patch, some of the individuals could jump again to another neighbouring patch. This could happen with species looking for places of higher prey densities, like mites, which disperse in the air and look for the best place to settle. In this work, the dispersal event is repeated k times, with all individuals leaving the patch where they are at each event. Therefore, insects fly at random from patch to patch without stopping for the total duration of the dispersal process. Then insects settle and thus can reach not only the closest neighbouring patches but also farther patches. Thus an increase of parameter k corresponds to a longer flight time.

Fig. 1 shows the spatial distribution after the dispersal process of insects initially located on a single patch for different values of k. The insect density is a Gaussian-like distribution, which corresponds to a diffusion pattern.

In recent works, Lett et al. [42,43] studied the effects of repeated dispersal events on the global dynamics of a host–parasitoid system (see also [44]). They considered a system of two spatial patches [42] and a row of patches [43] connected by dispersal. Local host–parasitoid interactions were described by the classical Nicholson–Bailey model, and hosts and parasitoids could disperse with constant proportions of migrants from one patch to another. This model involved two time scales, as between two generations the dispersal process could be repeated several times when the local interactions occurred only once. In the present work, we propose an extension of previous works to a square two-dimensional network of spatial patches (with A^2 patches) connected by dispersal. We compare the dynamics of the complete model (involving $2A^2$ variables for host and parasitoid local densities) to the aggregated model (involving only two variables, corresponding to the global host and parasitoid densities). Using aggregation methods, we investigate the effects of number of dispersal events and network dimension on the spatial synchrony of patches. We found that we need only a relatively small number of dispersal events to obtain a close match between the dynamics of the complete and the aggregated models.

2. Presentation and reduction of the model

The complete dynamics is a combination of two processes, a process of dispersal and a process of local host–parasitoid interactions.

2.1. The complete spatial model

In a homogeneous environment, the dynamics of host–parasitoid systems with discrete generations can be described by a pair of first-order difference equations (1)

$$\begin{cases} n_{t+1} = \lambda(n_t) n_t e^{-a p_t} \\ p_{t+1} = c n_t (1 - e^{-a p_t}) \end{cases} \tag{1}$$

which correspond to the Nicholson–Bailey model with host growth rate $\lambda(n_t)$. Here n_t and p_t are respectively the host and female parasitoid densities at generation t. For the host growth rate, we adopt the logistic form $\lambda(n_t) = \exp(r(1 - n_t/K))$, as first introduced by Beddington et al. [45], where r is a positive parameter and K is the carrying capacity. Therefore, in the absence of parasitoids, the host population would tend to K. Parameter a is the parasitoid searching efficiency and c is the average number of female parasitoids emerging from each infected host. If we suppose that the environment consists of a square lattice with $A \times A$ patches, the dynamics involves two phases. The first one corresponds to host–parasitoid interactions. Eq. (1) allow us to calculate local populations on each patch from one generation to the next. The second phase is dispersal between neighbouring patches. We assume that a constant proportion μ_n (resp. μ_p) of migrants for the host (resp. parasitoid) population is leaving any patch to go to the eight nearest patches in equal proportions. Eqs. (2) describe dispersal in a patch.

$$\begin{cases} n_{t+1} = (1 - \mu_n) n_t + \dfrac{\mu_n}{8} \sum_{\text{neighbours}} n_t \\ p_{t+1} = (1 - \mu_p) p_t + \dfrac{\mu_p}{8} \sum_{\text{neighbours}} p_t \end{cases} \tag{2}$$

In this model, we use reflexive boundaries, meaning that individuals moving out of the lattice will go back to the patch they come from (periodic boundaries would change the patterns obtained; however we found no influence on persistence). Under this condition, movements preserve the total numbers of hosts and parasitoids. The dispersal process for all the patches can be described by a non-negative matrix M. The complete model combines dispersal and local interactions as shown in Eq. (3).

$$X_{t+1} = F(M^k X_{t+1}) \tag{3}$$

The components of the $2A^2$-dimension vector X_t are the host and parasitoid densities on each patch. The vector of functions F is of the same dimension and incorporates the two previous equations of Eq. (1) of local insect interactions for all patches on the grid. Parameter k is an integer that we call dispersal frequency. When parameter $k = 1$, there is a single dispersal event between two generations. When $k > 1$, the dispersal process is repeated several times. Therefore, parameter k represents in a certain sense the ratio between the time scales of dispersal and local interactions. When k is increased, the dispersal process becomes faster with respect to local interactions. In this model, the dispersal process appears like a diffusion model (which steps are explicitly described). It can be seen as a one step migration which distributes individuals in an area around the starting patch, which is a compromise between the strict neighbourhood and the area covered by global migration. Parasitism occurs then in every patches where individuals have moved.

In the following sections, we will present simulations as examples. In most simulations, we will use the same set of parameters $a = 0.2$, $r = 2.6$, $K = 50$, and $c = 0.4$ to facilitate the comparison of simulation results. Furthermore, we use the values $\mu_n = \mu_p = 1$, i.e., every individual moves to an adjacent patch during each dispersal event. Henceforth, the set of parameters $a = 0.2$, $r = 2.6$, $k = 50$, $c = 0.4$, $\mu_n = \mu_p = 1$ will be referred to as the default set of parameters.

2.2. The aggregated model

For large values of k, an aggregated model is obtained in two steps. At the first step, we neglect the slow process of local host–parasitoids interactions and only study the fast dispersal process. With reflexive boundaries, there exists a positive and stable equilibrium of the dispersal process, which corresponds to the same proportion $1/A^2$ of hosts and parasitoids on each patch. This equilibrium corresponds to a spatially uniform distribution of hosts and parasitoids on the grid, and therefore to spatial synchrony among patches. In the second step an approximation is made. For any generation t, we assume that the system has reached the fast equilibrium due to the dispersal process before the slow dynamics, the local host–parasitoid interactions, takes place. Substituting the fast equilibrium into Eq. (1), and by summation of insect population densities for all patches of the grid, we obtain a reduced model (Eq. (4)) governing the dynamics of the total host density N_t and the total parasitoid density P_t at time t:

$$\begin{cases} N_{t+1} = N_t e^{\left(r(1-\frac{N_t}{KA^2})-\frac{a}{A^2}P_t\right)}, \\ P_{t+1} = cN_t(1 - e^{-\frac{a}{A^2}P_t}). \end{cases} \tag{4}$$

This model is also a Nicholson–Bailey model with host logistic growth. For a given set of parameters, the dynamics obtained for this model are the same as those obtained with Eq. (1), but with rescaling: if we define $u_t = N_t/A^2$ and $v_t = P_t/A^2$ and substitute them in Eq. (4), we obtain the system as the one defined by Eq. (1))

2.3. Comparison of the complete model and the aggregated model

We compare the dynamics of total host and parasitoid densities obtained with the complete model and with the aggregated model. As the number of dispersal events k increases, the dispersal process becomes fast in comparison to local interactions, and we expect the complete model dynamics to become 'closer' to the aggregated model one. In the examples to come, host and parasitoid population dynamics will be graphically represented as a phase portrait and the adequation of the dynamics can be evaluated qualitatively. But we also want to determine quantitatively how close the dynamics are.

Aggregation methods have mainly been developed in order to solve the complexity of models involving many state variables and parameters. Time scale separation methods take advantage of different time scales involved in the dynamics, to build by approximation methods a reduced model from the complete one. However, it is important to check that the dynamics of both models are close enough. This can be done in two main ways. First, one can check that, starting from the same initial condition, the solutions of the aggregated and complete models always remain close. For example, in [42], it was shown that for a two-patch model, an increase of parameter k allows

to maintain the distance between the trajectories of both models as small as expected. The same result holds for networks of larger dimensions. Another approach relates to the qualitative dynamics, i.e., the asymptotic behaviour of the complete and aggregated models. In the long term, after some transient dynamics during which the trajectories of the complete and aggregated models may differ, the solutions of the reduced model should tend for example to the same structurally stable attractor than those of the complete one. In this work, we pay a particular attention to this second aspect. We will see later a demonstrative example of the convergence of the complete model toward the asymptotic stable attractor of the aggregated model.

We use the sum of the variances V of host and parasitoid spatial distributions to compare the models. This coefficient gives a numerical determination of spatial uniformity of insect densities. A zero value corresponds to spatial uniformity. As we will see later, spatial uniformity corresponds to a similar asymptotic behaviour for the complete and aggregated models. When this coefficient tends to 0, spatial structures disappear and solutions of the reduced and complete model tend to the same structurally stable attractor.

We define a threshold value for V under which we consider that the density of hosts and parasitoids given by the complete model is uniform. We use here a value of 2, which corresponds to a mean difference of one host and one parasitoid per patch between the density distribution and the mean of densities, which is low compared to the carrying capacity of 50 hosts. We consider that the solution given by the complete model tends to the attractor of the aggregated model when the coefficient V drops and remains under this threshold.

3. Results

3.1. Effect of an increasing number of dispersal events on the spatial dynamics of the complete model

In this model, like in previous host–parasitoid spatial models [30,34,36], spatial structures like spiral waves can appear after a transient dynamics. The effect of an increasing number of dispersal events on the spatial structures of the host and parasitoid population densities is a kind of zoom effect, the spirals becoming larger. For even larger values of k, spiral waves may eventually vanish, leading to spatially uniform densities. To illustrate this phenomenon, we present in Fig. 2 the spa-

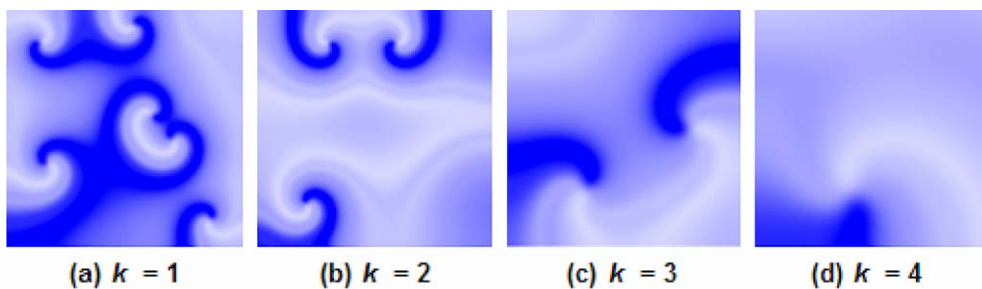(a) $k = 1$ (b) $k = 2$ (c) $k = 3$ (d) $k = 4$

Fig. 2. Numerical simulations of the complete model using the default set of parameters ($a = 0.2$, $r = 2.6$, $K = 50$, $c = 0.4$, $\mu_n = \mu_p = 1$) with $A = 200$. Number of hosts in each cell is portrayed at one generation, with the highest values in black.

tial patterns obtained for host population density with numerical simulations of the complete model (Eq. (3)) using the default set of parameters for increasing values of k. The initial condition corresponds to a few hosts and parasitoids located on a single patch and zero elsewhere, as found in Hassell et al. [30]. The influence of initial conditions will be discussed later. Following a transient dynamics, spiral waves are observed: for $k = 1$, there are six small spirals inside the network when only one bigger spiral remains for $k = 4$.

3.2. Comparison of the complete model and the aggregated model

The following examples will illustrate the behaviours of the complete and the aggregated models, and the incidence of parameter values on these.

3.2.1. Convergence of the trajectory of the complete model toward the attractor of the aggregated model

Fig. 3(a) presents numerical simulations of the aggregated model (Eq. (4)) for the same parameter values than in Fig. 2, but for a reduced grid ($A = 50$). After some transient dynamics that is not shown, the attractor of the aggregated model is a stable invariant curve, shown in black in Fig. 3(a). Fig. 3(b)–(d) present numerical simulations of the complete model for the default set of parameters and $k = 1$ at different time intervals: $0 < t < 500$ (b), $500 < t < 1000$ (c), and $1000 < t < 2000$ (d). At the beginning of the simulation, there were 20 hosts and parasitoids on one patch. To make the comparison between complete and aggregated models dynamics easier,
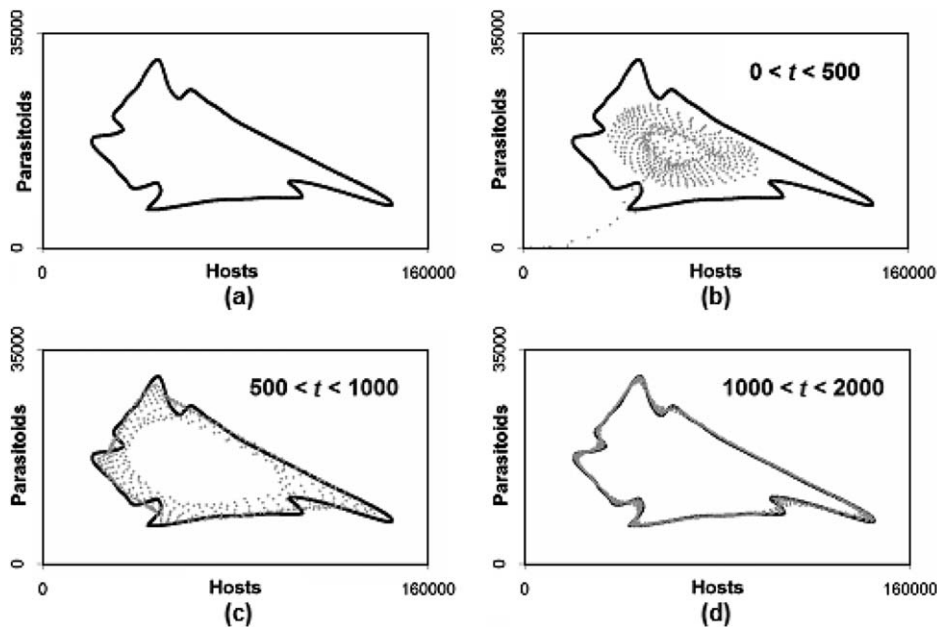

Fig. 3. (a) Numerical simulation of the aggregated model with $a = 0.2$, $r = 2.6$, $K = 50$, $c = 0.4$, $\mu_n = \mu_p = 1$ and $A = 50$. (b)–(d) Numerical simulation of the aggregated model like in (a) in black, and numerical simulation of the complete model for $k = 1$ in grey for $0 < t < 500$ (b), $500 < t < 1000$ (c) and $1000 < t < 2000$ (d).

the attractor of the aggregated model is shown in black and the solutions of the complete model are shown in grey. At each generation, the total host and parasitoid densities are calculated from the complete model (Eq. (3)) and also from the aggregated model (Eq. (4)). Observations of the complete model spatial dynamics showed that during a transient phase (not presented here), a spiral wave started but was not persistent. Although starting with the same initial condition, at the beginning the solutions are far apart during the transient dynamics, but after some generations the solutions of the complete and aggregated models tend to the same stable attractor. Fig. 3(d) shows that the trajectories of the complete model eventually converge to the attractor of the aggregated model.

3.2.2. Effect of the grid size

With a bigger grid ($A = 100$), the attractor of the aggregated model is similar to the one in the previous example. But for a movement frequency value of $k = 1$, contrary to the case of Fig. 3, a spiral wave invaded the grid and was persistent, and the solutions of the complete model did not converge to the attractor of the aggregated model (Fig. 4(a)). Fig. 4(b) shows that V remains large (about 200) and periodic for long simulation times.

3.2.3. Effect of the number of dispersal events

With the same set of parameters and the same initial condition as above, but with a larger value of k (here $k = 3$), the solution of the complete model tends to the attractor of the aggregated model, as shown in Fig. 4(c). In that case, a spiral wave could not persist. Spatial uniformity was observed all over the grid after a transient dynamics. Therefore, a larger value of k has permitted to
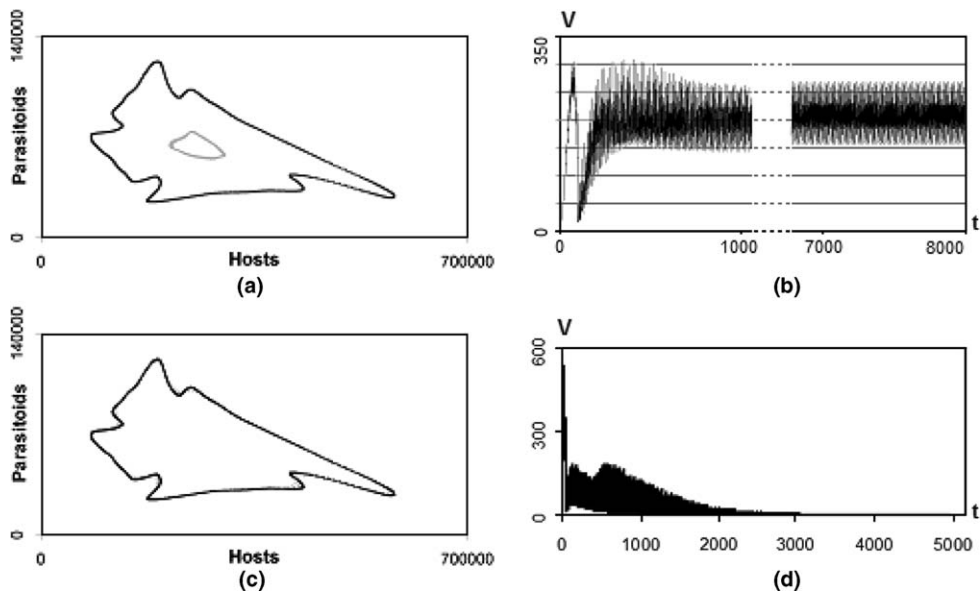

Fig. 4. Numerical simulations of the aggregated model (in black) and the complete model (in grey) with the default set of parameters and $k = 1$, $A = 100$ (a), and $k = 3$, $A = 100$ (c) for $1000 < t < 8000$. (b) and (d) represent the corresponding fluctuations of the sum of variances of hosts and parasitoids distribution V.

counter the effects of a bigger grid size. Fig. 4(b) shows that V tends to zero when $k = 3$, which means that the spatial patterns disappear. The fact that V drops and remains at low values is a good indicator of the disappearance of spatial structures like spirals, and also of the convergence of the complete model trajectories toward the attractor of the aggregated model.

Under very general conditions on function F, and when host and parasitoid populations are bounded, it can be shown that when k tends toward infinity, for any distribution of hosts and parasitoids at time t, the difference between the total population at time $t + 1$ for the complete and the aggregated model uniformly tends toward 0 (see the proof in Appendix A).

3.2.4. Effect of parameter r

We changed the parameter r to obtain models with different types of attractors. When $r = 2.15$ (other parameters being unchanged with respect to Fig. 3), the attractor of the aggregated model is periodic and corresponds to the five black dots shown in Fig. 5(a). For a movement frequency value of $k = 1$, unlike in case of Fig. 3, a spiral wave invaded the grid and was persistent, and the solutions of the complete model did not converge to the attractor of the aggregated model (result is not shown). Fig. 5(a), presents the comparison between the attractor of the aggregated model and the solutions of the complete model for $k = 2$. It shows that the solutions of the complete model tend to the attractor of the aggregated model. Spatial uniformity was observed all over the grid within less than 1500 generations. For $r = 2.94$, we obtain another attractor for the aggregated model (Fig. 5(b)). In this case, we only need $k = 1$ to get the convergence.

3.2.5. Sensitivity of convergence to initial conditions

To test the sensitivity of the complete model dynamics to initial conditions, we decided to consider three types of initial conditions, shown in Fig. 6. The first one (type (a)) consists of a small pack of hosts and parasitoids located close to the centre of the network, with location and number of individuals chosen at random. The second type (type (b)) consists of 20 pairs of hosts and parasitoids in one randomly chosen patch. This condition is similar to the one used in [30]. These two types of initial conditions could correspond to a group of insects colonizing a new area. The third type (type (c)) of initial conditions is a spiral obtained by running the model with parameters that lead to persistent spatial structures like in Fig. 2(a). Running repeated simulations with the default set of parameters, $A = 50$ and $k = 1$, we found that the complete model trajectories always
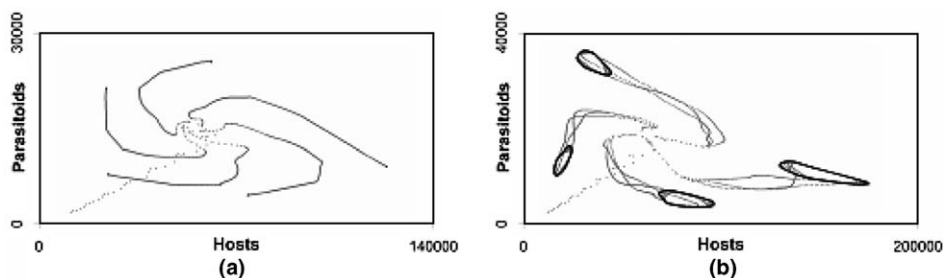

Fig. 5. Numerical simulation of the aggregated (black) and complete (grey) models in the same conditions as in Fig. 3 except $r = 2.15$ and $k = 2$ (a), and $r = 2.94$ and $k = 1$ (b).
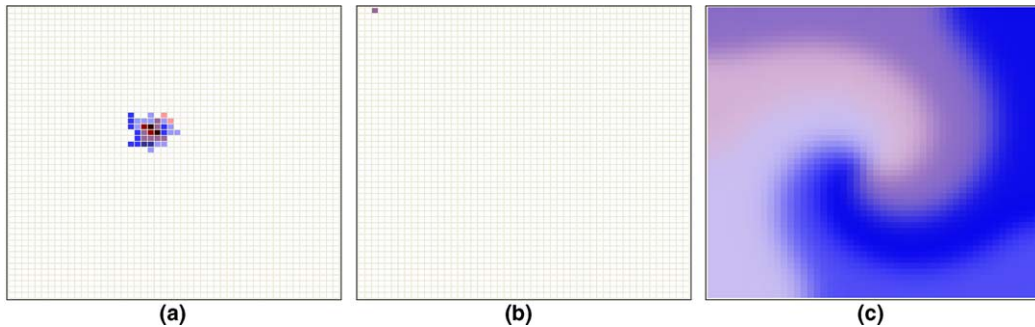
Fig. 6. Initial conditions used in those simulations: (a) pack of hosts and parasitoids in the centre of the grid, (b) one patch (randomly chosen) with 20 hosts and parasitoids and (c) spiral wave.

converged toward the attractor of the aggregated model with initial conditions type (b), but sometimes it did not with type (a) and never with type (c).

3.2.6. Critical dispersal frequency for convergence

The non-persistence of spatial structures when the parameter k is increased can be well understood from Fig. 2 showing that an increase of k provokes a zoom effect of spiral waves. For high enough values of the movement frequency, the two-dimensional grid is not large enough to support a persistent spiral wave. As a consequence, we suppose that there exists a threshold value $\tilde{k}$ of the k parameter below which spatial structures persist and above which they do not:

- if $k < \tilde{k}$, as long as we could check numerically, there are some cases where spatial structures persist, local dynamics remains asynchronous from patch to patch for very long simulation times and the aggregated model is not useful to make predictions about the dynamics of the complete model.
- if $k > \tilde{k}$, there exists a finite time such that spatial structures do not persist, the sum of variances of the host and parasitoid density distributions tends to zero, patch dynamics become synchronous and the aggregated model is useful to predict the asymptotic behaviour of the complete model, whatever the initial condition is.

We will now try to determine numerically the value $\tilde{k}$ for different sizes of grid and different sets of parameters. We have performed simulations for two-dimensional grids of dimension $A^2 = 900$, 2500, 10 000 and 40 000 and determined the influence of initial conditions and the proportion of migrants μ_n, μ_p on the behaviour of the system.

3.2.7. Determination of the critical value

To find a value of $\tilde{k}$ as independent on initial condition as possible, it is necessary to run many simulations with different initial conditions. The set of initial conditions types that were described previously permits us to determine a reasonable estimation of $\tilde{k}$.

To estimate the value of $\tilde{k}$ we performed several simulations using the default set of parameters. Precisely, for each value of k and A tested we performed 20 simulations with initial conditions type (a), 20 simulations with initial conditions type (b) and one simulation using initial condition

type (c). If for all simulations with the same initial condition type, the coefficient V dropped and stayed under the threshold value of 2 in less than 64,000 time steps, we noted a '+' in Table 1, otherwise we noted a '−'. It should be noted that when V was not below the threshold value at the end of a simulation it seemed to have reached a quasi-periodic state and was therefore unlikely to drop below it later.

For initial conditions (a) and $k = 1$, the complete model asymptotic dynamics is very different from the aggregated model one. However for larger values of k, the complete model behaves asymptotically like the aggregated model. We obtained significant differences in the results obtained for the three initial conditions types. While the solutions of the complete model tend to the attractor of the aggregated model for $k = 1$ with initial conditions (b) similar to that of Hassell et al. [30], we need a value of 3 to come to the same conclusion with condition (c). From Table 1 we choose the lowest value of k that assures a '+' for all the tested initial conditions as an estimation of $\tilde{k}$, i.e., $\tilde{k} = 3$. We assume that when using a value of k higher than $\tilde{k}$, the asymptotic dynamics for the complete model and the aggregated model will always be the same, whatever the initial condition is.

We repeated the simulations for a larger grid of size $A = 100$ (Table 2). The threshold value obtained in this case is $\tilde{k} = 8$. From Tables 1 and 2 we can see that initial condition of type (c) is the 'worst' as larger values of k are required in order to get a '+', even though we used only one simulation of this type while 20 of the other types. Therefore, for other grid sizes we decided to run only the simulation that uses initial condition of type (c) to determine the value of $\tilde{k}$ (Table 3).

The effect of k on the dynamics of the host–parasitoid system has also been investigated and the existence of a critical value has been found with other parameters values and other models like the classical Nicholson–Bailey model, which presents diverging local dynamics (no result shown).

Table 1
Results obtained for simulations with the default set of parameters and $A = 50$, for the three types of initial conditions

k	1	2	3	4	5	10
IC(a)	−	+	+	+	+	+
IC(b)	+	+	+	+	+	+
IC(c)	−	−	+	+	+	+

+ means that for all simulations performed, host and parasitoid distributions tend to spatial uniformity after some time, and − means that this was not the case for at least one simulation.

Table 2
Results obtained for simulations with parameters $a = 0.2$, $r = 2.6$, $K = 50$, $c = 0.4$, $A = 100$ and $\mu_n = \mu_p = 1$, and for the three initial conditions

k	1	2	4	7	8	9
IC(a)	−	+	+	+	+	+
IC(b)	−	+	+	+	+	+
IC(c)	−	−	−	−	+	+

Same as Table 1, except $A = 100$.

Table 3
Threshold values estimated for different sizes of grid

A	30	50	100	200
$\tilde{k}$	2	3	8	10

Table 4
Results for simulations with parameters $a = 0.2$, $r = 2.6$, $K = 50$, $c = 0.4$, and $A = 50$ for different values of $\mu = \mu_n = \mu_p$

μ	0.1	0.2	0.3	0.4	0.5	0.6	0.7	0.8	0.9	1
$\tilde{k}$	24	13	5	5	5	5	4	4	3	3
$\widetilde{\mu k}$	2.4	2.6	1.5	2	2.5	3	2.8	3.2	2.7	3

Second row: Threshold value for k above which spatial structures always disappear for initial condition (c). Third row: product $\widetilde{\mu k}$, indicator of the dispersal speed.

3.2.8. Effect of mobility μ

In the results shown previously, the proportion of migrants was set to 1. We expect the value of μ_n and μ_p to have an incidence on the threshold value $\tilde{k}$. In order to start an investigation on this point, we have studied the case where $\mu_n = \mu_p$ for other values between 0 and 1. We note $\mu = \mu_n = \mu_p$. We tested the hypothesis that there should be a threshold value $\widetilde{\mu k}$ under which spatial structures exist and above which they disappear. We have run simulations with parameters $a = 0.2$, $r = 2.6$, $K = 50$, $c = 0.4$ for a grid size $A = 50$ and initial condition (c) for different values of $\mu = \mu_n = \mu_p$, and have reported the results obtained in Table 4.

According to Table 4, for each value of the parameter μ, there is a value $\widetilde{\mu k}$ over which the solutions of the complete model converge to the attractor of the aggregated model. This value is roughly the same as the value of $\tilde{k}$ obtained for $\mu = 1$, i.e. about 3. Parameters μ and k have different consequences on dispersal: when μ increases, more individuals disperse, but still on the neighbouring patches, while when k increases, the individuals can reach further patches, the proportion of migrants being unchanged. However, those two parameters have roughly the same effect on the dynamics, as it is shown in Table 4.

4. Discussion and conclusion

In our model, insects are assumed to disperse several times per generation before reproduction. In classical models, Hassell et al. [30], insects disperse one time per generation and can only reach neighbouring patches, usually the eight closest patches. In our model, we assume that insects can go farther. In order to reach a non-contiguous patch, the insect must fly from the departure patch over several other patches which are located in between them. We have represented this dispersal process between two non-contiguous patches by a series of k dispersal events. Insects are assumed to fly at random in the network for a certain time and then can settle on a patch which can be more or less far from the departure patch. They can reach any patch located inside a disk of radius kL, where L is the average size of a patch. The spatial distribution that is obtained after a series of k dispersal events inside this domain resembles a Gaussian distribution as shown in Fig. 1. Thus in our work, dispersal model corresponds to a diffusion process, which may be seen as a compromise

between the one-step dispersal and the global dispersal which can be found in some other works (see Bernstein et al. [46,47]), where individuals are pooled and randomly distributed among the patches, moving implicitly several times.

In this work, we have shown that the aggregation method works for rather small values of parameter k, see Table 3. Therefore, the radius of this dispersal domain can be rather small and insects are assumed to disperse in a rather limited domain. As suggested to occur by French and Travis [48]: 'The parasitoids appeared to disperse more when larval host density was higher in the neighbouring cells than in the start cell. This is interesting because it is possible that individuals dispersed more than once during the dispersal period, and parasitoids visiting more than one cell may have been able to 'compare' local environments'. It is with this idea in mind that we conducted our work.

A lot of interest was devoted to the existence of spatial structures and mechanisms that facilitate their formation in host–parasitoid communities [49]. Spiral waves, spatial chaotic dynamics as well as crystalline structures have been obtained in modelling works. In these models, the patch model describing the local host and parasitoid interactions was unstable, as for example the classical Nicholson–Bailey model used in [30]. Instability came from the fact that a unique positive fixed point existed and was locally unstable for any set of parameter values. Therefore, in the case of a single isolated patch, after some generations the host density usually went to zero and consequently the parasitoid density too one generation after. In the case of a set of patches connected by dispersal, it was shown that the community could become persistent and that persistence was more likely to occur when the size of the spatial network was large. In this work, the patch model that we use, the Nicholson–Bailey model with host logistic growth, is not unstable. For some values of the parameters there can be a unique positive fixed point which is locally stable. For other values, stable attractors such as invariant curves or periodic attractors can occur. In the case of a network of patches connected by dispersal, our numerical simulations have shown that spatial structures can also be observed and can be persistent. Fig. 2 shows spiral waves similar to the ones described in [30,34].

Our work has shown that there exists a threshold value of the movement frequency k above which spatial patterns do not persist and patch dynamics become synchronous. In such cases, an aggregated model governing the total insect population densities can be obtained and is successful to make suitable predictions about the dynamics of the complete model. The existence of a threshold value of k is not unexpected. Indeed, diffusion tends to reduce spatial gradients and to promote spatial homogeneity. Therefore, when dispersal events become more frequent, a homogeneous spatial state is more likely to occur. Thus, for a high value of k, one can understand that the proportion of hosts and parasitoids become similar from patch to patch, destroying spatial structures and inducing spatial synchrony. However, it is unexpected that the critical value of the k parameter is relatively low. Our simulations have shown that for networks of 10 000–40 000 patches, a value of 8–10 dispersal events per generation is enough to promote spatial synchrony. In such situations, individuals disperse within a disk which radius is about 5–10% of the size of the square grid side, which corresponds to a rather short range of dispersion with respect to habitat size. As a consequence, for realistic ranges of dispersion, it is possible to build an aggregated model that can provide useful information about the macroscopic asymptotic behaviour of the complete model. That means that in most cases, local diffusion is enough to destroy spatial structures and to lead to spatial synchrony.

We showed that fast dispersal can favour spatial synchrony. However, we did not take into account stochastic processes, which on the contrary can induce spatial asynchronous dynamics. Local environmental variability, which may be different from patch to patch, would also favour spatial asynchrony. With correlated environmental disturbance (Moran effect), the population synchrony would be exactly the same than the environment synchrony for linear models [50]. Abiotic factors such as climatic or habitat heterogeneity can provide such variability [51], while in this paper only biotic factors have been taken into account. Both factors should be taken in consideration as their respective roles are still unclear [52]. Furthermore, we focused here on a fixed proportion of dispersing individuals. We have now to consider density-dependent dispersal: local density of individuals may have either a positive or a negative effect on dispersal, and then on dynamics and synchrony [48]. In reality several factors operate at the same time and may have different and even opposite effects on spatial synchrony. The balance between these different factors is probably a key factor to explain the resulting observed host–parasitoid spatial dynamics.

Our work was oriented toward host–parasitoid communities. In the near future, we would like to extend it to other kinds of models (continuous time models), other spatial communities (predator–prey models) and other species (birds, fishes...). Therefore, our work could propose a general framework for the study of spatial synchrony based on aggregation of variables.

Appendix A

A.1. The complete model

Let us consider the following complete model for a grid with A^2 cells

$$\begin{cases} n_{t+1} = f(M_n^k n_t; M_p^k p_t) \\ p_{t+1} = g(M_n^k n_t; M_p^k p_t) \end{cases}$$

where A is the size of one side of the grid, $n_t, p_t \in \mathbb{R}^{A^2}$ are vectors representing host and parasitoid populations in every patch at time step t, f and g are functions C^1 of $\mathbb{R}^{2A^2}$ in $\mathbb{R}^{2A^2}$ corresponding to the local dynamics. The movement frequency k is a positive integer and M_n and M_p are $A \times A$ dispersal matrix for hosts and parasitoids such as for each column, the sum of elements is equal to 1 (stochastic matrix). We consider matrix that are irreducible and aperiodic, which is the case for dispersal on the eight nearest neighbours with a constant proportion of migrants on a square grid.

Let us consider the $2A^2$-dimension vector X_t defined by $X_t = (n_t, p_t)^T \in \mathbb{R}^{2A^2}$ which contains population densities for hosts (A^2 first elements) and for parasitoids (A^2 last elements). We introduce the function $h = (f; g)^T$ and the matrix of dispersal $M = \text{diag}(M_n; M_p)$. We can now write the complete model like in Eq. [2]

$$X_{t+1} = h(M^k X_t)$$

Let $\mathbf{1}$ be a A^2 vector which elements are all equal to 1, and $\tilde{\mathbf{1}} = \text{diag}(\mathbf{1}^T; \mathbf{1}^T)$. The function $\tilde{\mathbf{1}}hM^k$ gives for any population vector X_t a 2-dimension vector which elements are total population for hosts and parasitoids at time step $t + 1$.

A.2. The aggregated model

Let us consider $\overline{M} = \lim_{k \to +\infty} M^k$.

Let $\overline{v_n}$ be the eigen vector of norm 1 associated to the eigen value 1 of M_n, and $\overline{v_p}$ the eigen vector of norm 1 associated to the eigen value 1 of M_p. We denote $\bar{v} = (\overline{v_n}; \overline{v_p})^{\mathrm{T}}$.

For all population vectors n_t and p_t, we have $\lim_{k \to +\infty} M_n^k n_t = (\mathbf{1}^{\mathrm{T}} n_t) v_n$ (Perron–Frobenius theorem) and $\lim_{k \to +\infty} M_p^k p_t = (\mathbf{1}^{\mathrm{T}} p_t) v_p$.

By defining $S = \mathrm{diag}(\overline{v_n}; \overline{v_p})$ we have

$$S\tilde{\mathbf{1}} = \overline{M}$$

Let us consider the vector in $\mathbb{R}^2$ representing hosts and parasitoids total populations $(u_t; v_t)^{\mathrm{T}}$ to which we associate the following population vector:

$$(n_t; p_t)^{\mathrm{T}} = (u_t \overline{v_n}; v_t \overline{v_p})^{\mathrm{T}}$$

we have

$$(u_{t+1}; v_{t+1})^{\mathrm{T}} = (\mathbf{1}^{\mathrm{T}} n_{t+1}; \mathbf{1}^{\mathrm{T}} p_{t+1}) = (\mathbf{1}^{\mathrm{T}} f(M_n^k n_t; M_p^k p_t); \mathbf{1}^{\mathrm{T}} g(M_n^k n_t; M_p^k p_t))$$

Because we consider the system to be at fast equilibrium, we approach $M^k V_t$ with $\overline{M} V_t = (u_t \overline{v_n}; v_t \overline{v_p})^{\mathrm{T}}$, and we obtain

$$(u_{t+1}; v_{t+1})^{\mathrm{T}} = (\mathbf{1}^{\mathrm{T}} f(u_t \overline{v_n}; v_t \overline{v_p}); \mathbf{1}^{\mathrm{T}} g(u_t \overline{v_n}; v_t \overline{v_p}))$$

We then define the aggregated model as follows

$$\begin{cases} u_{t+1} & = F(u_t; v_t) \\ v_{t+1} & = G(u_t; v_t) \end{cases}$$

with $F(u_t; v_t) = \mathbf{1}^{\mathrm{T}} f(u_t \overline{v_n}; v_t \overline{v_p})$ and $G(u_t; v_t) = \mathbf{1}^{\mathrm{T}} g(u_t \overline{v_n}; v_t \overline{v_p})$.

A.3. Approximation of total population given by the aggregated model

Let us denote $H = (F; G)^{\mathrm{T}}$. We can then write

$$H = \tilde{\mathbf{1}} h S$$

For any population vector X_t, the vector of total population is given by $(u_t; v_t)^{\mathrm{T}} = \tilde{\mathbf{1}} X_t$. Then the approximation of total population given by the aggregated model at the next timestep is

$$(u_{t+1}; v_{t+1})^{\mathrm{T}} = H(\tilde{\mathbf{1}} X_t) = \tilde{\mathbf{1}} h S(\tilde{\mathbf{1}} X_t)$$

Because $S\tilde{\mathbf{1}} X_t = \overline{M} X_t$, we have

$$(u_{t+1}; v_{t+1})^{\mathrm{T}} = \tilde{\mathbf{1}} h(\overline{M} X_t)$$

A.4. Result

We give to the space $\mathbb{R}^{2A^2}$ a norm $\|.\|$. We suppose that there exists a compact K of $\mathbb{R}^{2A^2}$ such as the dynamics stay in that compact $(h(K) \subset K)$ and such as h is C^1 on that compact. Then for any

distribution X_t, the difference between total populations calculated with the complete model and the aggregated model after one timestep tends toward 0 when k tends to infinity. More precisely:

$$||\tilde{\mathbf{1}}hM^k - H\tilde{\mathbf{1}}|| = \mathrm{O}\left(\frac{1}{k}\right)$$

Proof. For any population vector X_t in K, the distance between the total population given by complete and aggregated model is

$$||\tilde{\mathbf{1}}h(M^kX_t) - H(\tilde{\mathbf{1}}X_t)|| = ||\tilde{\mathbf{1}}h(M^kX_t) - \tilde{\mathbf{1}}h(\overline{M}X_t)|| \leqslant ||\tilde{\mathbf{1}}||.||h(M^kX_t) - h(\overline{M}X_t)||$$

because h is C^1 on K, there exists $\alpha \in \mathbb{R}$ such as h is α-lipschitz. Then

$$||\tilde{\mathbf{1}}h(M^kX_t) - H(\tilde{\mathbf{1}}X_t)|| \leqslant \alpha||\tilde{\mathbf{1}}||.||M^kX_t - \overline{M}X_t|| \leqslant \alpha||\tilde{\mathbf{1}}||.||M^k - \overline{M}||.||X_t||$$

Because X_t is in a compact, we have for any X_t

$$||\tilde{\mathbf{1}}h(M^kX_t) - H(\tilde{\mathbf{1}}X_t)|| \leqslant \mathrm{constant}||M^k - \overline{M}||$$

and so

$$||\tilde{\mathbf{1}}hM^k - H\tilde{\mathbf{1}}|| \leqslant \mathrm{constant}||M^k - \overline{M}|| = \mathrm{O}\left(\frac{1}{k}\right)$$

References

[1] I. Hanski, I.P. Woiwod, Spatial synchrony in the dynamics of moth and aphid populations, J. Anim. Ecol. 62 (1993) 656.

[2] J.H. Myers, Synchrony in outbreaks of forest lepidoptera: a possible example of the Moran effect, Ecology 79 (1998) 1111.

[3] E. Ranta, V. Kaitala, J. Lindström, H. Lindén, Synchrony in population dynamics, Proc. R. Soc. London 262 (1995) 113.

[4] I.M. Cattadori, S. Merler, P.J. Hudson, Searching for mechanisms of synchrony in spatially structured gamebird populations, J. Anim. Ecol. 69 (2000) 620.

[5] E. Paradis, S.R. Baillie, W.J. Sutherland, R.D. Gregory, Spatial synchrony in population of birds: effect of habitat, population trend, and spatial scale, Ecology 81 (2000) 2112.

[6] R.A. Ims, H.P. Andreassen, Spatial synchronization of vole population dynamics by predator birds, Nature 408 (2000) 194.

[7] E. Ranta, V. Kaitala, J. Lindström, Dynamics of Canadian lynx populations in space and time, Ecography 20 (1997) 454.

[8] M. Chaloupka, Historical trends, seasonality and spatial synchrony in green turtle egg production in the southeast Asian region, Biol. Conserv. 101 (2001) 263.

[9] W.D. Koenig, J.M.H. Knops, Scale of mast-seeding and tree-ring growth, Nature 396 (1998) 225.

[10] B.M. Bolker, B.T. Grenfell, Impact of vaccination on the spatial correlation and persistence of measles dynamics, Proc. Natl. Acad. Sci. USA 93 (1996) 12648.

[11] A.R.E. Sinclair, J.M. Gosline, G. Holdsworth, C.J. Krebs, S. Boutin, J.N.M. Smith, R. Boonstra, M. Dale, Can the solar cycle and climate synchronise the snowshoe hare cycle in Canada? Evidence from tree rings and ice cores, Am. Nat. 141 (1993) 173.

[12] E. Ranta, J. Lindström, H. Lindén, Synchrony in tetraonid population dynamics, J. Anim. Ecol. 64 (1995) 767.
[13] E. Ranta, J. Lindström, V. Kaitala, H. Kokko, H. Lindén, E. Helle, Solar activity and hare dynamics: a cross-continental comparison, Am. Nat. 149 (1997) 765.
[14] P.J. Hudson, I. Cattadori, The Moran effect: a cause of population synchrony, Trends Ecol. Evol. 14 (1999) 1.
[15] G.D. Ruxton, P. Rohani, Fitness dependent dispersal in metapopulations and its consequences for persistence and synchrony, J. Anim. Ecol. 67 (1998) 530.
[16] B.J. Sawnson, D.R. Johnson, Distinguishing causes of intraspecific synchrony in population dynamics, Oikos 86 (1999) 265.
[17] S. Muratori, S. Rinaldi, Low and high-frequency oscillations in three-dimensional food chain systems, SIAM J. Appl. Math. 52 (1992) 1688.
[18] S. Rinaldi, S. Muratori, Limit cycles in slow-fast forest pest models, Theor. Populat. Biol. 41 (1992) 26.
[19] S. Rinaldi, S. Muratori, Slow-fast limit cycles in predator–prey models, Ecol. Model. 61 (1992) 287.
[20] Y. Iwasa, V. Andreasen, S.A. Levin, Aggregation in model ecosystems. I. Perfect aggregation, Ecol. Model. 37 (1987) 287.
[21] Y. Iwasa, S.A. Levin, V. Andreasen, Aggregation in model ecosystems. II. Approximate aggregation, IMA J. Math. Appl. Med. Biol. 6 (1989) 1.
[22] S.A. Levin, S. Pacala, Theories of simplification and scaling of spatially distributed processes, in: D. Tilman, P. Kareiva (Eds.), Spatial Ecology: The Role of Space in Population Dynamics and Interspecific Interactions, Princeton University, 1997, p. 271.
[23] S. Pacala, S.A. Levin, Biologically generated spatial patterns and the coexistence of competing species, in: D. Tilman, P. Kareiva (Eds.), Spatial Ecology: The Role of Space in Population Dynamics and Interspecific Interactions, Princeton University, 1997, p. 204.
[24] P. Auger, R. Roussarie, Complex ecological models with simple dynamics: from individuals to populations, Acta Biotheor. 42 (1994) 111.
[25] P. Auger, J.C. Poggiale, Aggregation and emergence in systems of ordinary differential equations, Math. Comput. Model. 27 (1998) 1.
[26] O. Arino, E. Sanchez, R. Bravo de la Parra, P. Auger, A model of an age-structured population with two time scales, SIAM J. Appl. Math. 60 (1999) 408.
[27] R. Bravo de la Parra, E. Sanchez, O. Arino, P. Auger, A discrete model with density dependent fast migration, Math. Biosci. 157 (1999) 91.
[28] P. Auger, R. Bravo de la Parra, Methods of aggregation of variables in population dynamics, C. R. Acad. Sci. III 323 (2000) 665.
[29] C.J. Briggs, M.F. Hoopes, Stabilizing effects in spatial parasitoid–host and predator–prey models : a review, Theor. Populat. Biol. 65 (2004) 299.
[30] M.P. Hassell, H.N. Comins, R.M. May, Spatial structure and chaos in insect population dynamics, Nature 353 (1991) 255.
[31] J.C. Allen, Mathematical models of species interactions in time and space, Am. Nat. 109 (1975) 319.
[32] P. Rohani, G.D. Ruxton, Dispersal-induced instabilities in host–parasitoid metapopulations, Theor. Populat. Bio. 55 (1999) 23.
[33] J.D. Reeve, Environmental variability, migration, and persistence in host–parasitoid models, Am. Nat. 132 (1988) 810.
[34] H.N. Comins, M.P. Hassell, R.M. May, The spatial dynamics of host–parasitoid systems, J. Anim. Ecol. 61 (1992) 735.
[35] F.R. Adler, B. Nuernberger, Persistence in patchy irregular landscapes, Theor. Populat. Biol. 45 (1994) 41.
[36] P. Rohani, O. Miramontes, Host–parasitoid metapopulations: the consequences of parasitoid aggregation on spatial dynamics and searching efficiency, Proc. R. Soc. London B 260 (1995) 335.
[37] J.M.J. Travis, D.R. French, Dispersal functions and spatial models: expanding our dispersal toolbox, Ecol. Lett. 3 (2000) 163.
[38] G.D. Ruxton, Synchronisation between individuals and the dynamics of linked populations, J. Theor. Biol. 183 (1995) 47.
[39] H.C.J. Godfray, Parasitoids. Behavioral and Evolutionary Ecology, Princeton University, 1994.

[40] M.E. Hochberg, A.R. Ives, Parasitoid Population Biology, Princeton University, 2000.

[41] Y. Huang, O. Diekmann, Double jump migration and diffusive instability, Bull. Math. Biol. 66 (2004) 487.

[42] C. Lett, P. Auger, R. Bravo de la Parra, Migration frequency and the persistence of host–parasitoid interactions, J. Theor. Biol. 221 (2003) 639.

[43] C. Lett, P. Auger, F. Fleury, Effect of asymmetric dispersal and environmental gradients on the stability of host–parasitoid systems, Oikos 109 (2005) 603.

[44] C. Bernstein, P. Auger, J.C. Poggiale, Predator migration decisions, the ideal free distribution and predator–prey dynamics, Am. Nat. 153 (1999) 267.

[45] J.R. Beddington, C.A. Free, J.H. Lawton, Dynamics complexity in predator–prey models framed in difference equations, Nature 255 (1975) 58.

[46] C. Bernstein, A. Kacelnik, J.R. Krebs, Individual decisions and the distribution of predators in a patchy environment, J. Anim. Ecol. 57 (1988) 1007.

[47] C. Bernstein, A. Kacelnik, J.R. Krebs, Individual decisions and the distribution of predators in a patchy environment. II. The influence of travel costs and structure of the environment, J. Anim. Ecol. 60 (1991) 205.

[48] D.R. French, J.M.J. Travis, Density-dependent dispersal in host–parasitoid assemblages, Oikos 95 (2001) 125.

[49] P. Rohani, T.J. Lewis, D. Grünbaum, G.D. Ruxton, Spatial self-organisation in ecology: pretty patterns or robust reality? Trends Ecol. Evol. 12 (1997) 70.

[50] J. Rippa, Analysing the Moran effect and dispersal: their significance and interaction in synchronous population dynamics, Oikos 89 (2000) 175.

[51] L.E. Loe, C. Bonenfant, A. Mysterud, J.M. Gaillard, R. Langvatn, F. Klein, C. Calenge, T. Ergon, N. Pettorelli, N.C. Stenseth, Climate predictability and breeding phenology in red deer: timing and synchrony of rutting and calving in Norway and France, J. Anim. Ecol. 74 (2005) 579.

[52] B.K. Singh, J. Subba Rao, R. Ramaswamy, S. Sinha, The role of heterogeneity on the spatiotemporal dynamics of host–parasite metapopulation, Ecol. Model. 180 (2004) 435.